Integrated fuzzy guidance law for high maneuvering targets based on proportional navigation guidance

L. Hassan, S. H. Sadati, and J. Karimi.

Abstract: An integrated fuzzy guidance (IFG) law for a surface to air homing missile is introduced. The introduced approach is a modification of the well-known proportional navigation guidance (PNG) law. The IFG law enables the missile to approach a high maneuvering target while trying to minimize control effort as well as miss-distance in a two-stage flight. In the first stage, while the missile is far from the intended target, the IFG tends to have low sensitivity to the target maneuvering seeking to minimize the overall control effort. When the missile gets closer to the target, a second stage is started and IFG law changes tactic by increasing that sensitivity attempting to minimize the miss-distance. A fuzzy-switching point (FSP) controller manages the transition between the two stages. The FSP is optimized based on variety of scenarios; some of which are discussed in the paper. The introduced scheme depends on line-of-sight angle rate, closing velocity, and target-missile relative range. The performance of the new IFG law is compared with PNG law and the results show a relative superiority in wide variety of flight conditions.

Keywords: Fuzzy Logic, Homing Missile, Proportional Navigation Guidance.

Nomenclature

T	Target
M	Missile
LOS	Line-of-sight.
V_C	The T-M closing velocity.
λ	LOS angle.
$\dot{\lambda}$	LOS rate.
A_T	T acceleration.
A_M	M acceleration.
A_C	M acceleration command.
V_T	T velocity.
V_M	M velocity.
R_{TM}	T-M relative range.
R_{TM1}	T-M vertical range.
R_{TM2}	T-M horizontal range.
γ_M	M flight path angle.
γ_T	T flight path angle.
C_{EFF}	Control Effort.
M_D	Miss Distance.

1 Introduction

In the last two decades, developing appropriate guidance laws, which remain suitable for intercepting missiles in wide varieties of flight conditions, have attracted considerable attentions. This mainly emerges in the case of highly maneuverable aircrafts, for which conventional approaches may not be sufficient to obtain both tracking and interception, unless there is a perfect knowledge about the system dynamics and also extensive computational capabilities are available. The conventional approaches to this subject include: Exact feedback linearization [1], [2], Sliding mode control [3], [4], Adaptive control [5], [6], and the last not the least LQ-based control system [7], [8]. It is therefore appropriate to investigate other advanced control theories to improve existing performance capabilities. In this line of thought, Fuzzy logic controllers have shown to exhibit suitable properties which help eliminating measurement deficiencies or other difficulties such as changing climatic conditions. This could help open a new approach for control system design.

In fact; most fuzzy guidance laws are implemented based on the well-known classical guidance laws; especially PNG law which enjoys simplicity, effectiveness and ease of implementation [9], [10]. In

Iranian Journal of Electrical & Electronic Engineering,
The Authors are with the department of Aerospace Engineering, Maleke Ashtar University of Technology, Tehran, Iran.
E-mails: lab.has77@yahoo.com, hsadati@aut.ac.ir, karimi_j@alum.sharif.edu

general, PNG controller remains a good choice against low maneuvering targets [11], while such approach cannot provide satisfactory performance and robustness with respect to high maneuvering targets and results large value of M_D because of dynamic saturation at the end game [12]. Designers solve this problem by modifying the PNG law to an augmented proportional navigation guidance APNG one. This is achieved by adding a term of the target acceleration into the PNG law, the matter that enables PNG controller to be more effective against highly maneuvering targets. On the other hand, adding the corresponding term means there has to be an ability to estimate the target acceleration instantaneously which may not always be available. To overcome this difficulty an integrated fuzzy guidance controller namely IFG is proposed. It is based on the concept of PNG law and consists of two autonomous fuzzy controllers. Each of the two controllers has its own characteristics; together they can achieve the interception. An FSP controller is designed to switch between the two fuzzy controllers. The first fuzzy controller namely FG1 is designed to be with low sensitivity to the target maneuvering trying to minimize the control effort (C_{EFF}) and would be used in the first stage of flight where the missile is far from its target. Whereas, the second fuzzy controller, denoted by FG2, is designed to have higher sensitivity to target's maneuvering trying to minimize the miss distance (M_D) when the missile becomes closer to its target.

The paper is organized as follows: We proceed with a brief overview of the PNG law in Section 2, whereas; IFG controller with its three components FG1, FG2, and FSP is explained in Section 3. We provide some case-studies in Section 4 and the differences of all guidance laws are discussed. Finally, in Section 5 we discuss some important conclusions.

2 An Overview on PNG Law.

For problem formulation, we use point mass. The missile and target are moving with constant velocities where drag and gravitational effects are neglected. The engagement scenario is shown in Fig. 1.

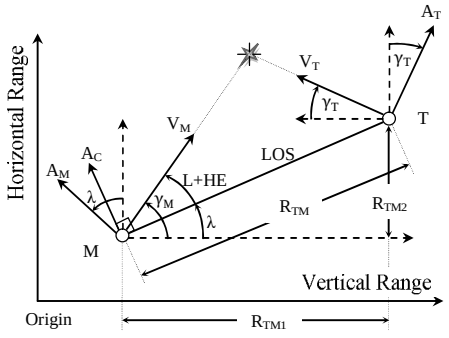

Fig. 1: Two-dimensional missile-target engagement geometry.

In vertical plane, the closing velocity V_C which is negative rate of the missile target range can be written as:

$$V_C = -\dot{R}_{TM} \cong V_M - V_T \quad (1)$$

Where:

$$\dot{R}_{TM} = -\frac{R_{TM1}V_{TM1}+R_{TM2}V_{TM2}}{R_{TM}} \quad (2)$$

The Line of Sight (LOS) angle λ and its rate $\dot{\lambda}$ can be given as:

$$\lambda = \tan^{-1}\left(\frac{R_{TM1}}{R_{TM2}}\right) \quad (3)$$

$$\dot{\lambda} = \frac{R_{TM1}V_{TM2}-R_{TM2}V_{TM1}}{{R_{TM}}^2} \quad (4)$$

Theoretically; PNG as used in many missiles gives the commanded acceleration perpendicular to the instantaneous LOS, the magnitude being proportional to the LOS rate and the closing velocity as:

$$A_C = NV_C\dot{\lambda} \quad (5)$$

A missile employing PNG law usually aims toward expected interception point. Theoretically, a missile will reach its target if both of missile and the target continue flying along a straight-line path at constant velocities. However, this idealized assumption is violated for high maneuvering targets [13]. That is because when the missile gets closer and closer to a maneuvering target, LOS starts changing very rapidly which in turn causes very large $\dot{\lambda}$ values. With acceleration command being proportional to $\dot{\lambda}$ values, as in Eq. (5), the matter could eventually lead to some form of dynamic saturation; resulting large M_D. A fuzzy controller is expected to provide a desirable solution through modifying PNG. This prevents such undesirable scenarios that would arise from unwanted system saturations.

3 Architecture of Integrated Fuzzy Guidance (IFG) Law:

The main idea behind the proposed IFG law is to use relatively small acceleration commands while the missile is far from the target, where high maneuvers would not achieve a better performance regarding a maneuvering target; so we prefer to save C_{EFF}. On the other hand, the acceleration command could be increased sensibly as soon as the missile gets closer to its target to deliver good tracking capability and to decrease M_D.

The entire proposed structure is shown in Fig. 2, with three main components; FG1, FG2, and FSP. The

heart of the system is, in fact; the FSP controller which needs to be tuned to ensure smooth transition between FG1and FG2.

Assuming two weights referred to as w_1 and w_2 define how long either of FG1 and FG2 are engaged and how the transition between the two is moderated. We now elaborate on the details.

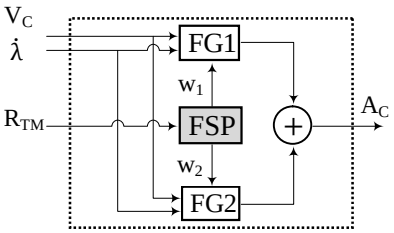

Fig. 2: The IFG controller.

Each controller FG1, FG2, and FSP has alike structure that illustrated in Fig. 3.

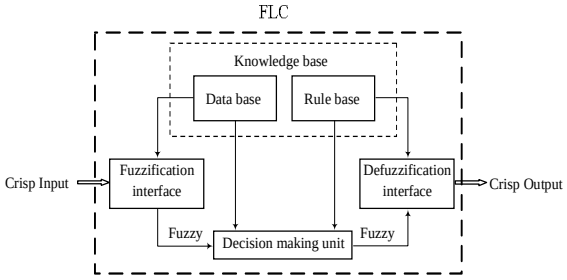

Fig. 3: Fuzzy inference system.

Fuzzy inference systems are composed of five functional blocks [14]. These are; a rule base containing a number of if-then rules, a database that defines the membership functions (MFs), a decision making interface which operates the given rules, a fuzzification interface that converts the crisp inputs into "degree of match" with the linguistic values like small or large etc., and a defuzzification interface which reconverts to a crisp output.

Different case-studies reveal that for the current work, the center of area (CoA) method, which supplies defuzzified output with better continuity, is more effective [15], [16]. Furthermore; Minimum Mamdani (AND method), the most popular inference engine, provides good results and allows easy and effective computation with real time capability [17].

The first step to design a fuzzy controller is to choose number and shapes of the MFs for input and output. Actually; there is no rigid restrictions on the number of MFs. Determined the number and the shape of MFs is a compromise between guidance accuracy and computation complexity.

In this work; three groups of MFs with triangular shape are investigated for each of the controllers FG1 and FG2. Using other more complex forms of MFs would not give any significant advantage over the triangular ones [18], we further show that the triangular MFs even give faster response. Similar to PNG law, the inputs of both controllers FG1 and FG2 are both V_C and $\dot{\lambda}$ whereas the output is A_C. That is each controller exploits two groups of MFs corresponding to the inputs whereas the third group is used for the output. Each group has seven MFs where each MF is denoted by a linguistic value. The linguistic values can be represented as :{ LN, MN, SN, ZE, SP, MP, LP}, where "L", "M", and "S" represent "Large", "Medium", and "Small" respectively. Similarly; "N", "ZE", and "P" denote "Negative", "Zero", and "Positive" respectively.

The FSP controller receives R_{TM} as its input and gives two weights (w_1, w_2) on its outputs. The input in turn has two MFs; Small "S" and Large "L" with bell-shaped MFs to insure smooth transition whereas each output has two triangular MFs.

The data of each controller are normalized according to max method normalization [19]. This method divides the performance ratings of each attribute (r) by its maximum performance rating (r_{max}). The normalization procedures are required to transform performance ratings with different data measurement units into a decision matrix with compatible unit. In our design the maximum values are obtained based on the knowledge available about missile dynamic in addition to previous experiences about other classical guidance laws in PNG's class.

Finally; we need to define the rules that organize the relationship between the control action and missile-target measurements. Here; the rules are determined according to the PNG law. In fact, the choice of proper MFs and rules requires a great deal of engineering intuition and so it could be considered as some type of engineering art. We provide some more explanation of the process in the next sections.

3.1 Search for Proper Rules:

Fuzzy Logic, in the first glance, looks simple and straightforward; nonetheless, like every engineering process complexities arise as we proceed further into the design. This work is not an exception; here we aim to find a set of proper rules that allow guiding a missile toward its target in a two-stage flight. One must note to the point that, both FG1 and FG2 have similar rules and MFs serve as input to them. The process to define the rules and the MFs is explained in the following statements.

With Eq. (5), the acceleration command A_C of PNG law is proportional to $\dot{\lambda}$ multiplied by V_C. So, one might argue that the sign of A_C remains negative; as long as $\dot{\lambda}$ or V_C have opposite signs. Therefore, we could prepare a table such as Table 1.

Table 1 Defining the sign of $\mathbf{A_C}$.

If	V_C	is	N	and	$\dot{\lambda}$	is	P	then	A_C	is	N
If	V_C	is	N	and	$\dot{\lambda}$	is	N	then	A_C	is	P
If	V_C	is	P	and	$\dot{\lambda}$	is	P	then	A_C	is	P
If	V_C	is	P	and	$\dot{\lambda}$	is	N	then	A_C	is	N

Again, we need to normalize all information in the interval of [-1, 1] before feeding them into the controller. It is further noted that, multiplication of any two variables in this interval would result in a value which is smaller than the smallest value among them, whereas at the same time it is closer to the relatively smaller one of the two. In addition; the output would be zero if either of inputs were zero. This is similar to Minimum Mamdani type mechanism (AND method) which has been used in the existing design process. Adopting these concepts, the linguistic A_C values could be defined based on Table 2:

Table 2 Defining the value of $\mathbf{A_C}$.

If	V_C	is	L	and	$\dot{\lambda}$	is	L	then	A_C	is	L
If	V_C	is	L	and	$\dot{\lambda}$	is	M	then	A_C	is	M
If	V_C	is	L	and	$\dot{\lambda}$	is	S	then	A_C	is	S
If	V_C	is	L	and	$\dot{\lambda}$	is	ZE	then	A_C	is	ZE
If	V_C	is	M	and	$\dot{\lambda}$	is	L	then	A_C	is	M
If	V_C	is	M	and	$\dot{\lambda}$	is	M	then	A_C	is	M
If	V_C	is	M	and	$\dot{\lambda}$	is	S	then	A_C	is	S
If	V_C	is	M	and	$\dot{\lambda}$	is	ZE	then	A_C	is	ZE
If	V_C	is	S	and	$\dot{\lambda}$	is	L	then	A_C	is	S
If	V_C	is	S	and	$\dot{\lambda}$	is	M	then	A_C	is	S
If	V_C	is	S	and	$\dot{\lambda}$	is	S	then	A_C	is	S
If	V_C	is	S	and	$\dot{\lambda}$	is	ZE	then	A_C	is	ZE
If	V_C	is	ZE	and	$\dot{\lambda}$	is	L	then	A_C	is	ZE
If	V_C	is	ZE	and	$\dot{\lambda}$	is	M	then	A_C	is	ZE
If	V_C	is	ZE	and	$\dot{\lambda}$	is	S	then	A_C	is	ZE
If	V_C	is	ZE	and	$\dot{\lambda}$	is	ZE	then	A_C	is	ZE

Taking into account the two previous concepts enables us to find the necessary rules (Table 3):

Table 3 The rules.

A_C		$\dot{\lambda}$						
		LP	MP	SP	ZE	SN	MN	LN
V_C	LP	LP	MP	SP	ZE	SN	MN	LN
	MP	MP	MP	SP	ZE	SN	MN	MN
	SP	SP	SP	SP	ZE	SN	SN	SN
	ZE	ZE	ZE	ZE	ZE	ZE	ZE	ZE
	SN	SN	SN	SN	ZE	SP	SP	SP
	MN	MN	MN	SN	ZE	SP	MP	MP
	LN	LN	MN	SN	ZE	SP	MP	LP

These rules are, in fact, describing PNG law in a fuzzy domain and exhibit almost similar behavior to the PNG when using similar shapes of MFs for both inputs and output.

3.2 Defining MFs:

As mentioned previously, the controllers FG1 and FG2 have similar rules and similar input MFs. Since the rules are derived, the MFs of the inputs ($\dot{\lambda}$ and V_C) are adjusted using test and error method and plotted as following:

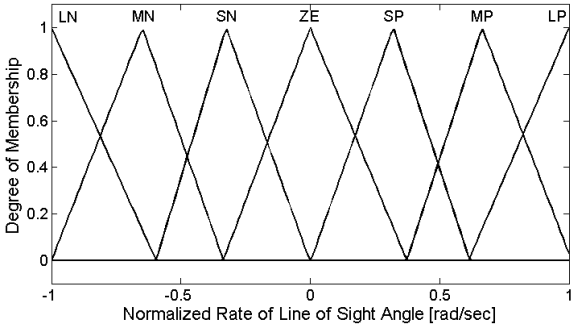

(a) MFs of rate of LOS angle

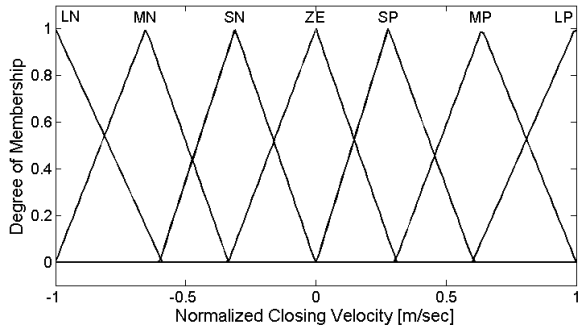

(b) MFs of the closing velocity

Fig. 4: Input MFs for both FG1 and FG2.

The last remained part is to investigate the output MFs under the consideration; FG1 has to ensure low sensitivity and FG2 has to ensure high sensitivity.
In this regard; we say FG1 is more sensitivity than FG2 when both controllers are fed with same input value and FG1 is able to give larger output value than FG2.
Actually, the output value can be controlled by three factors; shape of MFs, number of MFs, and CoA location. Investigations showed that CoA location has much more effecting among the other factors [15]. So, the output value will be controlled by shifting the location of the CoA respect to Zero Point (ZP). Where the increasing is achieved by displacing CoA far from ZP and decreasing is carried out by displacing it toward ZP. The following figured example demonstrates the process.

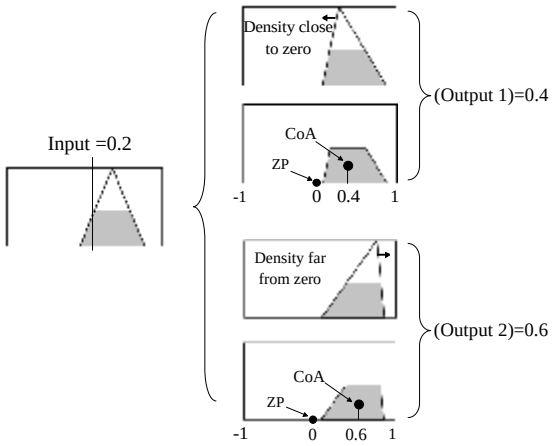

Fig. 5: Effect of CoA displacement on the output values.

With Fig. 5; suppose FG1 has output MF with density close to ZP whereas FG2 has output MF with density far from ZP. Feeding input value equals to 0.2 for both controllers, FG1 gives output value equals to 0.4 whereas FG2 gives output value equals to 0.6. It is clear that for same input value, FG2 can give greater output value.

Based on the previous illustration; we can insure FG1 with low sensitivity by pressing the output MFs toward ZP which in turn shifts the CoA of each MF toward ZP and decreases the acceleration command values. In turn; decreasing the acceleration command leads to decrease the guidance law sensitivity the mater that causes C_{EFF} conserving.

On the other hand; spreading the output MFs of FG2 far from ZP leads to shift the CoA of each MF far from ZP and increases the acceleration command value which in turn increases the guidance law sensitivity the mater that causes small M_D.

Fig. 6 shows the shape of output MFs for the both controllers FG1 and FG2.

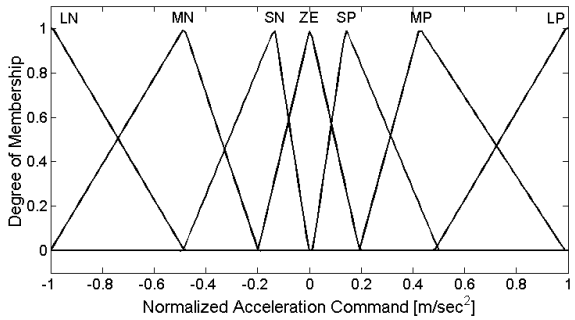

a. The output MFs of FG1 with density close to ZP.

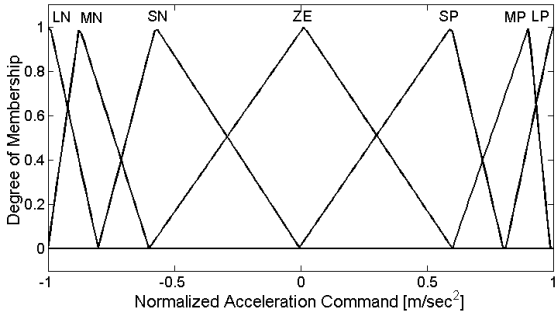

b. The output MFs of FG2 with density far from ZP.

Fig. 6: Output MFs

3.3 The FSP controller:

The FSP controller has single input R_{TM} and two outputs (w_1, w_2), the rules of this controller are simply determined as following:

- If R_{TM} is large then w_1 is large and w_2 is small.
- If R_{TM} is small then w_1 is small and w_2 is large.

The first rule refers to FG1 domination whereas the second rule refers to FG2 domination. The FSP insures the integration between the two controllers and balances the dominance of FG1 and FG2.

3.3.1 MFs of the FSP controller:

The integration is achieved by transition from FG1 to FG2 via the weights w_1 and w_2. The weights in turn are changed respect to the input MFs which define the transition way. Since FG1 has to give low A_C values and FG2 has to give large ones, a sudden transition will force the missile to change maneuvering in high rates, the matter could cause target missing or even bending the missile body. MFs that have broken shapes (e.g., Triangular) are main reason of a sudden change because of its corners whereas MFs with smooth curves (e.g., Bell-shaped) can avoid the hasty transition. So, Bell-shaped MFs are used for FSP input. Since the input MFs insure the smooth transition between w_1 and w_2, both the weights have to insure the exact values "0" and "1", otherwise, undesirable coupling between FG1 and FG2 will happen before and after switching.

Anyway, we will discuss the smooth transition via the input MFs in a separate section whilst the ability of insuring the exact values "0" and "1" will be shown currently.

Actually, the exact values "0" and "1" are achieved by adjusting output triangular MFs as close as possible to the terminals, therein the values "0" and "1" are located (e.g., "Fig. 5").

It is notable to point that an opposite result occurs when expanding the MFs far from the terminals, where the output values become somewhat more than "0" or

less than "1", the matter that causes undesirable mix between FG1 and FG2 before or after switching.

Fig. 7, which plotted as an example, shows how the adjusting close to the terminals can insure the exact values "0" or "1". In the drawing, we consider that, for the input (R_{TM} = 0.7), the switching from FG1 to FG2 is completed. So that, it supposed to have complete-inert FG1 and complete-energetic FG2.

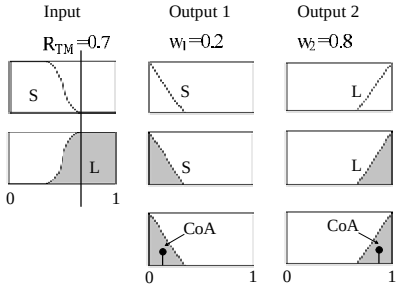

Case (a) MFs adjusting far from terminals.

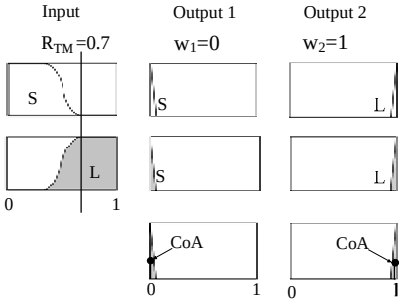

Case (b): MFs adjusting close to terminals.

Fig. 7: MFs adjusting respect to the terminals.

Case (a) shows that the MFs are not adjusted close to terminals. Therefore, the outputs are $w_1 = 0.2$ and $w_2 = 0.8$, this means a coupling still existent between FG1 and FG2 even after finishing the transition. By adjusting the MFs close to terminals, as shown in Case (b), the outputs become as possible as the values "0" and "1" respectively, ensuring no-coupling (complete-inert and complete-energetic).

3.3.2 Optimizing input MFs:

Since we insured the undesirable coupling, it is turn to achieve an optimal transition using the input Bell-shaped MFs. In fact; the generalized MFs depends on three parameters **a**, **b**, and **c**, given as following:

$$F(x, \mathbf{a}, \mathbf{b}, \mathbf{c}) = \frac{1}{1+\left|\frac{x-c}{a}\right|^{2b}} \quad (6)$$

Where; x denotes degree of the MF, **a** controls the width of the curve, **b** controls its slope and **c** control its center. The transition between the two controllers appears clearly in Fig. 8. Before transition, FG1 is complete-energetic and FG2 is complete-inert, therein; $w_1 = 1$and $w_2 = 0$. When switching starts, FG2 begins to share FG1 smoothly whilst FG1 remains dominator. In this interval w_1 decreases and w_2 increases until the weights become equal each to other at point (P). Thereafter, the process is reversed and FG2 becomes dominator. The process continues till we have, $w_1 = 0$ and $w_2 = 1$, thereon the switching is completed.

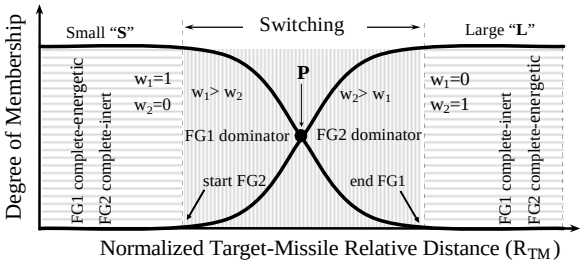

Fig. 8: MFs of input

The location of P and the slope of the MFs are managing the entire work of the IFG controller and the best tuning of these MFs the best performance of the IFG controller. For this purpose, an algorithm using MatLab software is investigated. The algorithm has two main steps; in the first one we define ***When*** the transition will be, upon that the algorithm sifts the location of P which recognized by the parameters (**a**, **c**). Whereas the assessment of the slope is achieved in the next step based on the parameter (**b**) that defines *How* the transition will be. Fig. 9 illustrates the overall process of the algorithm.

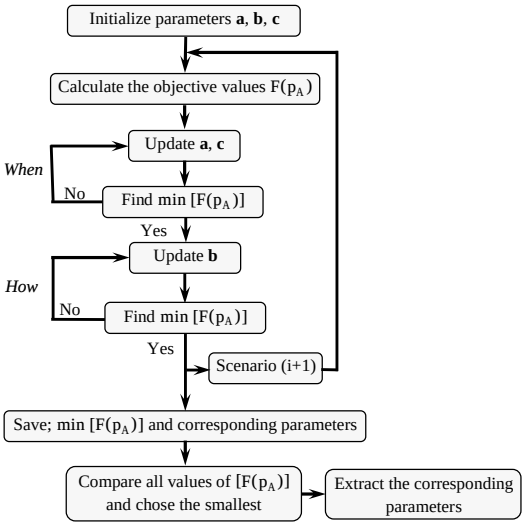

Fig. 9: Flowchart of the optimization algorithm.

The algorithm is run for variety different scenarios of target maneuvering. In each scenario the minimum

value of the objective function is calculated. The calculated value and its corresponding parapets are saved. All saved values of the object functions are compared. The parameters that cause smallest value of the object function among all scenarios are extracted as an optimal solution.

The object function includes two terms; C_{EFF} and M_D and calculated as following:

$$F(p_A) = k_1 . \int_0^{t_f} {A_C}^2 dt + k_2 . R_{TM}(t_f) \quad (7)$$

Where: p_A is the array's parameters needed to be optimized, t_f is the entire time of flight, k_1 and k_2 are designed constants refer to the terms preference C_{EFF} and M_D. In our design we considered same importance for both of the terms, so that; $k_1 = 1/A_{C_{max}}$, $k_2 = 1/R_{TM(t_f)_{max}}$, where $A_{C_{max}}$ and $R_{TM(t_f)_{max}}$ are the maximum allowable values of the acceleration and the miss distance respectively.

Running the simulation for variety of extreme scenarios, the algorithm calculates the optimal parameters of FSP controller. The parameters are extracted and listed as below:

Table 4 Tuned parameters of the SFP.

MFs	**a**	**b**	**c**
S	0.508	8.31	-0.15
L	0.507	8.29	0.85

3 Result and analysis:

For the simulation we provide the following considerations:

The initial positions of the target and the missile are $(0, 0)\,\mathrm{km}$, $(8, 3)\mathrm{km}$ respectively. $V_M = 1000\,(\mathrm{m.sec^{-1}})$, $V_T = 300\,(\mathrm{m.sec^{-1}})$. The target can accelerate within $[-3, 8]\mathrm{g}$, whereas the missile can accelerate within $[-20, 20]\mathrm{g}$, where $g = 9.8(\mathrm{m.sec^{-2}})$ is the gravity constant. The navigation ratio of PNG law is $N = 4$.

The general arrangement of the guidance loop is illustrated in Fig. 10.

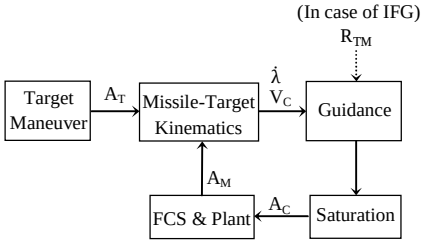

Fig. 10: Homing Guidance Loop.

With the help of [20], the transfer function of flight control system (FCS) and the plant is presented as:

$$\frac{A_M}{A_C} = \frac{-0.006S^2+11.296}{0.003S^3+0.139S^2+3.42S+11.313} \quad (8)$$

One of the important factors in the simulation process is usually the integration time-step. This is normally chosen based on nature of the problem or experience. Here, we use a time step equal to 0.01 second, mainly because a typical missile-gyro gyrates around 100 cycles per second. Additional important factor is that simulation stop condition; with Eq. (1), we can note that V_C will be zero when R_{TM} that denotes the resulting M_D is extrumum (e.g., the function is either minimum or maximum when its derivative is zero), therein the simulation will stop.

To complete the work, the maximum values needed for normalizing are simply calculated basing on Eq. (1) as well as Eq. (5) and tabulated as following:

Table 5 Maximum values for normalization.

Substantives	Calculated	Max values
A_C	20×9.8	197 [m/sec^2]
V_C	$1000 + 300$	1300 [m/sec]
$\dot{\lambda}$	$(20 \times 9.8)/(4 \times 1300)$	0.038 [rad/sec]

Engagement accuracy of all prior guidance laws against 24 different scenarios is examined. The scenarios are simulated respect to the target acceleration $A_T = [-3, -2, \ldots, 7, 8]\mathrm{g}$, as well as its movement direction (incoming or evading). Since we cannot show all scenarios, four selected scenarios respect to maximum capability of the target maneuvering are chosen and plotted as following.

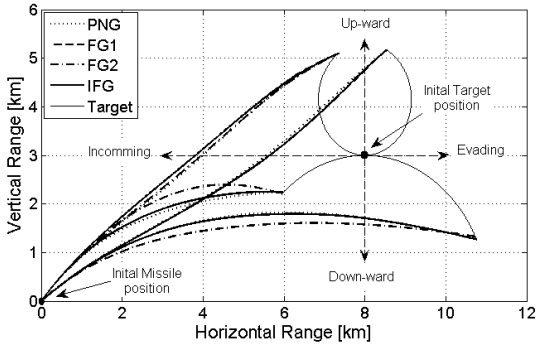

Fig. 11: Trajectories of selected scenarios.

The selected scenarios are achieved for the following target maneuvering styles; Incoming Up-ward, Incoming Down-ward, Evading Up-ward, and Evading Down-ward. Fig. 11 shows that using PNG or IFG enables to intercept the maneuvering target. In addition it shows that even using FG1 or FG2 can insure the interception regardless of the resulting M_D or C_{EFF}.

The acceleration histories, respects to each selected scenario, are separately illustrated as following.

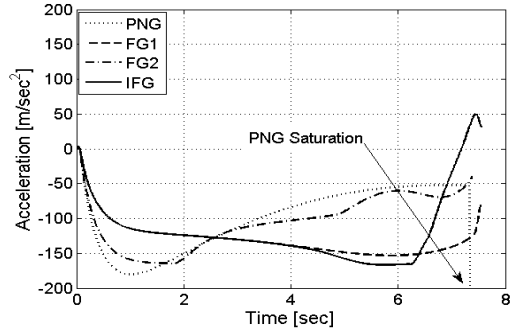

a. Incoming Down-ward maneuvering.

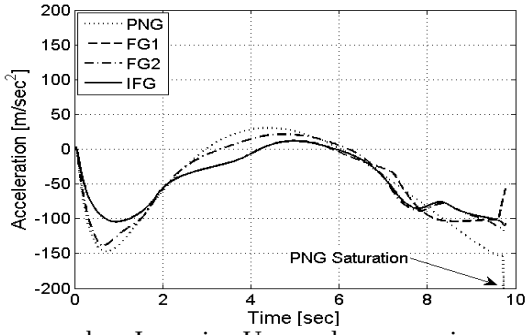

b. Incoming Up-ward maneuvering.

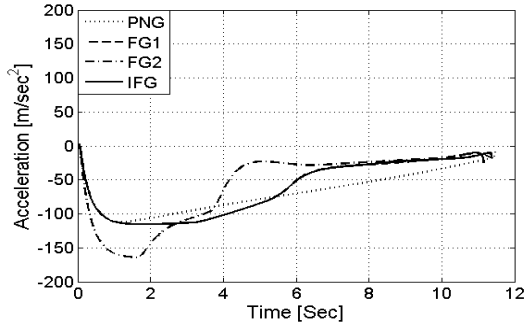

c. Evading Down-ward maneuvering.

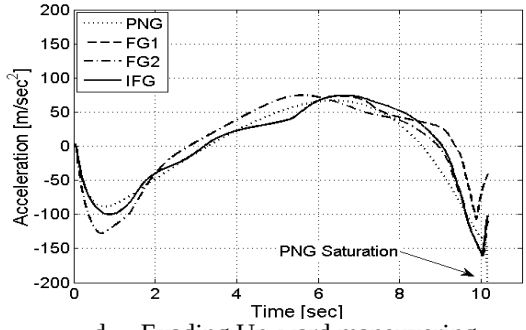

d. Evading Up-ward maneuvering.

Fig. 12: Accelerations histories for different maneuvering styles.

With Fig. 12, acceleration command histories show that there saturation could be happen during the endgame for PNG such as Fig. 12 (a, b, c), the matter that causes M_D increasing. Also it displays the smooth transition from FG1 to FG2.

The root-mean-square values (RMS) for the overall 24 scenarios are listed in Table 6.

Table 6 RMS of M_D and C_{EFF} for 24 scenarios.

RMS	M_D [m]	C_{EFF} [10^{-4} $m^2.sec^{-3}$]
FG1	7.86	5.36
FG2	5.13	6.84
IFG	5.43	5.84
PNG	7.21	6.52

Table 6 declares that FG1law shows its best capability to conserve the C_{Eff} compared to the other ones, nonetheless; it gives the highest M_D value. On the other hand, the Table shows that the high sensitive FG2 has the best capability to achieve the smallest M_D value, but causes the highest C_{Eff} value.

The most interesting outcome, which results from integrating both controllers by the optimized FSP, is the IFG law which overcomes the PNG law in terms of M_D and C_{Eff} together, not alike FG1 or FG2 those achieve overcoming in one of the two terms. The following figure plots the resulting, M_D and C_{Eff} for the overall 24 scenarios in details.

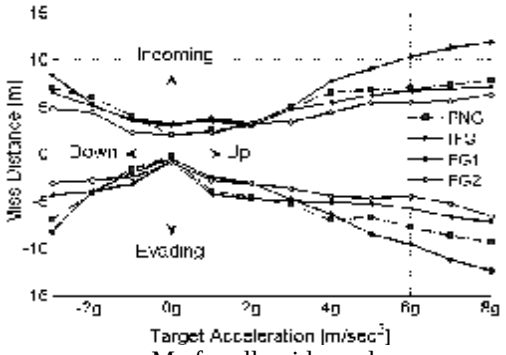

a. M_D for all guidance laws.

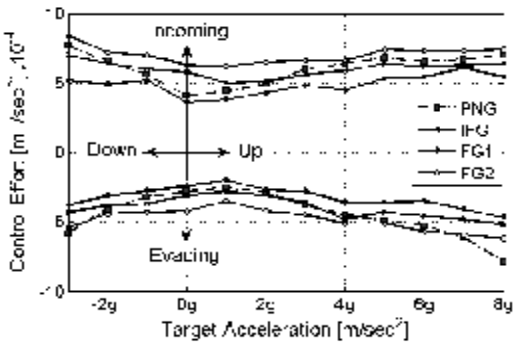

b. C_{EFF} for all guidance laws.

Fig. 13: M_D and C_{EFF} for the all guidance laws.

Fig. 13 that compares PNG law with the other ones in terms of M_D and C_{Eff} verifies the results given in Table 6 and shows the following conclusions:

- FG1 law with low sensitivity is appropriate to conserve the C_{Eff} and shows better behavior in case of low target maneuvering, approximately when ($|A_T| < 2g$). On the other hand it achieves the worst when the target maneuvers sharply ($|A_T| > 2g$).
- FG2 law with high sensitivity is appropriate when small M_D is desirable and shows good behavior for high target maneuvering. Whereas, it causes higher C_{Eff} spending.
- IFG law which is an integral of the two prior fuzzy guidance laws seems to be perfect for all scenarios. In total, IFG law overcomes PNG law in term of both C_{Eff} and M_D. It is notable to mention that sign this kind of guidance laws enables to avoid the saturation that maybe happen while using PNG law which in turn increases the M_D and the C_{Eff}.

Basing on the previous results we can say that; three phases guidance (initial, midcourse, and terminal) are not always necessary. In fact, we can have two-phases fuzzy guidance combined of a low-sensitive phase and a high-sensitive one those have the characteristics mentioned previously. Furthermore; we can show that, under such condition low C_{Eff} demand, we can suffice to have FG1. And under the condition low M_D desire, we can use FG2, the matter that very helpful from practical point of view. That is a single set of gains is enough when a fast response is necessary.

Noise affecting on IFG:

It is well-known that measuring a target location follows a random distribution due to thermal and radar noises; therefore, white noise is added to the measured signals to account for the disturbances. Such effects can be modeled as Gaussian density function (G_{df}) declared as:

$$G_{df}(n_s) = \frac{1}{\sqrt{2\pi\sigma^2}} . e^{-\frac{(x-\mu)^2}{2\sigma^2}} \qquad (9)$$

Where; μ is the noise mean value and σ is its standard deviation, whereas n_s is the noiseless signal. Using the MtLab function ***awgn***, we add white Gaussian noise to the input signals and evaluate the RMS of M_D and C_{EFF}. The calculation is achieved for three different levels of signal-to-noise ratio (SNR). The resulted values are tabulated as following:

Table 7 Performance of IFGL with noise existence.

SNR	RMS of M_D [m]	RMS of C_{EFF} [10^{-4} m^2/sec^3]
100	8.87	7.57
50	13.22	10.66
25	1162.61	5.02

Table 7 shows that as the noise increases the missile interception capability decreases. That is because of noisy information was send to the guidance law which in turn send confused commands to the flight control system.

From practical point of view, the proposed design shows acceptable performance with the existence of noise, where the resulting M_D and C_{EFF}, in case of SNR > 50 are allowable in nowadays' missiles [11].

4 Conclusion:

In this work, we have investigated the possibilities of developing an IFG law with two subcomponents FG1 and FG2. The investigation is based on a modification of classical PNG law. Simulation for variety scenarios of target maneuvering is achieved for a surface to air homing missile which dynamically described by a transfer function.

RMS of the terms M_D and C_{EFF} is calculated for all scenarios. FG1 with low sensitivity to the target maneuvering is investigated to insure small C_{EFF} values regardless of M_D whereas FG2 concerns on minimizing M_D only. The results show that both FG1 and FG2 enable the missile to track and intercept the target. Since FG1 relatively causes C_{EFF} conserving and M_D increment, FG2 diametrically does the opposite. Each of the subcomponents overweighs PNG law in one of the terms M_D or C_{EFF}. By motivating FG1 and slacking FG2 in the early flight stages, and vise versa in the last stages, an integration of the two subcomponents can be achieved. The resulted IFG shows better performance than PNG law in both terms. FSP controller secures an optimal transition between the two controllers. The FSP is optimized by an algorithm which defines when and how the transition would be done. Many cases have been examined for different scenarios. Since PNG law tends to show saturation in many scenarios, the other guidance laws do not show any saturation. Further investigations proved that the IFG shows acceptable performance in case of high SNR values. Nevertheless, further investigation maybe achieved to develop the current design in case of low SNR levels.

References

[1] B. T. Burchett, "Feedback linearization guidance for approach and landing of reusable launch vehicles" American Control Conference, vol. 3, pp. 2093 – 2097, 2005.

[2] C. C. Kung, F. L. Chiang, and K. Y. Chen, "Design A Three-dimensional pursuit guidance law with Feedback Linearization Method" World Academy of Science, Engineering and Technology, vol. 79, pp. 136-141, 2011.

[3] F. K. Yeh, H. H. Chien, and L. C. Fu, "Design of optimal midcourse guidance sliding-mode control for missiles with TVC" IEEE Trans. on Aerospace and Electronic Systems, vol. 39, no. 3, pp. 824-837, 2003.

[4] R. M. Shoucri, "Closed Form Solution of Line-of-Sight Trajectory for Maneuvering Target" AIAA

Journal of Guidance, Control, and Dynamics, vol. 24, no. 2, pp. 408-409, 2001.
[5] C. M. Lin and Y. F. Peng, "Missile guidance law design using adaptive cerebellar model articulation controller" IEEE Trans. Neural Network, vol. 16, no. 3, pp. 636-644, 2005.
[6] Stepanyan, V., and Hovakimyan, N., "Adaptive disturbance rejection controller for visual tracking of a maneuvering target" Journal of Guidance, Control, and Dynamics, vol. 30, no. 4, pp. 1090-1106 , 2007.
[7] J. I. Lee, I. S. Jeon, and M. J. Tahk, "Guidance law to control impact time and angle" IEEE Aerospace and Electronic Systems, vol. 43, no. 1, pp. 301-310, 2007.
[8] Savkin, A. V., Pathirana, P., and Faruqi, F. A., "The Problem of Precision Missile Guidance: LQR and H_∞ Frameworks" IEEE Transactions on Aerospace and Electronic Systems, vol. 39, no. 3, pp. 901–910, 2003.
[9] DS. Deshkar, MM Kuber, and PP Parakhi, "Fuzzy logic guidance law with optimized membership function" International Journal of Computer Science and Informatics, vol. 1, no 2, pp 52-56, 2011.
[10] V. Rajasekhar and A. G. Sreenatha, "Fuzzy Logic Implementation of Proportional Navigation Guidance" Acta Astronautica, vol. 46, no. 1, pp.17-24, 2000.
[11] Siouris, G., "Missile Guidance and Control Systems" Springer, New York, NY, 2004.
[12] P Zarchan, "Tactical and Strategic Missile Guidance" 5th edition, AIAA, 2007.
[13] Lin C.L., and Chen Y.Y., "Design of Fuzzy Logic Guidance Law against High Speed Target" Journal of Guidance, Control and Dynamics, vol. 23, no.1, January-February, pp. 17-25, 2000.
[14] J. S. R. Jang, "Adaptive-Network-Based Fuzzy Inference system" IEEE Transactions on Systems, Man, and Cybernetics, vol. 23, no. 3, pp. 665-685, 1993.
[15] Werner Van Leekwijck and Etienne E. Kerre, "Defuzzification: criteria and classification" Fuzzy Sets and Systems, vol. 108, pp. 159-178. 1999.
[16] J. Lindblad and N. Sladoje. "Feature Based Defuzzification at Increased Spatial Resolution" Proc., of 11th Intern. Workshop on Combinatorial Image Analysis, Berlin, Germany, Lecture Notes in Computer Science, vol. 4040, pp. 131-143, 2006.
[17] B. S. U. Mendis, T. D. Gedeon, J. Botzheim, L. T. Koczy "Generalized Weighted Relevance Aggregation Operators for Hierarchical Fuzzy Signatures" International Conference on Computational Intelligence for Modeling Control and Automation, 2006.
[18] C. L. Lin, H. Z. Hung, Y. Y. Chen, and B. S. Chen, "Development of an Integrated Fuzzy logic based missile guidance law against high speed target" IEEE, Transaction on Fuzzy System, vol. 12, no. 2, 2004.
[19] S. Chakraborty and C. Yeh. "A Simulation Based Comparative Study of Normalization Procedures in Multi-attribute Decision Making." The 6th WSEAS Int. Conf. on Artificial Intelligence, Knowledge Engineering and Data Bases, Corfu Island, Greece, pp. 102-109, 2007.
[20] Chun Ling Lin, Tzu Chiang Kao, and Meng Tzong Wu, "Design of a Fuzzified Terminal Guidance Law," International Journal of Fuzzy Systems, vol. 9, no. 2, pp. 110-115, 2007.

Seyed Hossein Sadati is an Assistant Professor in the Department of Aerospace Engineering at Maleke Ashtar University of Technology, Tehran, Iran. Dr. S.H Sadati received his Ph.D. in Aerospace Engineering from Amirkabir University in 2008. He has published more than 25 journal and conference papers in the area of Aerospace Engineering. His current research interests include the control system design for aircraft, trajectory optimization, nonlinear control, optimal control, neural network and fuzzy Control.

Jalal Karimi is an Assistant Professor in the Department of Aerospace Engineering at Maleke Ashtar University of Technology, Tehran, Iran. Dr. Karimi received his Ph.D. in Aerospace Engineering from Sharif University of Technology in 2012. His current research interests are Motion planning and heuristic optimization.

L. Mahmoud Hassan is currently a PHD student in the Department of Aerospace Engineering at Maleke Ashtar University of Technology, Tehran, Iran.